

Structural and Optical Properties of Pure NiO Nanoparticles and NiO-Mn₂O₃, NiO-CdO, NiO-Pb₂O₃, NiO-ZnO Nanocomposites

E. J. Vishaka^a, M. Priya Dharshini^b, V. Shally^b and Sr. Gerardin Jayam^b

^a Research Scholar (Reg.No:20213042132010), Research Department of Physics, Holy Cross College, Nagercoil – 629004. Affiliated to Manonmaniam Sundaranar University, Abishekapatti, Tirunelveli- 627012, India.

^b Research Department of Physics, Holy Cross College, Nagercoil – 629004.

Doi: <https://doi.org/10.47011/14.5.2>

Received on: 01/05/2020;

Accepted on: 25/1/2021

Abstract: Pure nickel oxide (NiO) nanoparticles and NiO-Mn₂O₃, NiO-CdO, NiO-Pb₂O₃, NiO-ZnO nanocomposites were synthesized by co-precipitation method. The PXRD studies revealed that NiO, Mn₂O₃ and CdO possessed cubic structure, Pb₂O₃ possessed monoclinic structure, ZnO possessed hexagonal structure and confirmed the presence of polycrystallinity nature of NiO and Mn₂O₃, CdO, Pb₂O₃, ZnO in the nanocomposites. The average grain size of NiO nanoparticles was found to be 30.10 nm using Debye Scherer's formula. The FESEM images of NiO nanoparticles and their nanocomposites revealed spherical shaped structure and NiO-Pb₂O₃ revealed needle shaped rod-like structure. EDAX analysis confirmed the composition of NiO nanoparticles and their nanocomposites. Raman spectra exhibited characteristic peaks of pure NiO and that of NiO-Mn₂O₃, NiO-CdO, NiO-Pb₂O₃, NiO-ZnO in the synthesized nanocomposites. In the PL spectra, blue and green emission was observed in the samples. UV-vis spectra revealed the absorption peaks of NiO nanoparticles and their nanocomposites. Thus, the synthesized NiO-Mn₂O₃, NiO-CdO, NiO-Pb₂O₃ and NiO-ZnO nanocomposites can be a suitable material for electrocatalysis applications.

Keywords: Nickel oxide nanocomposites, Structure, Morphology, Absorption, Luminescence.

1. Introduction

Nickel oxide (NiO) is an important transition metal oxide that has been under the extensive investigation for decades due to its interesting electronic structures, strongly affected by Ni-3d electrons [1] which are localized in space, but spread out over a wide energy range because of strong Coulomb repulsion between them [2]. The high specific surface area of NiO nanoparticles has significant implications with respect to the energy storage devices based on electrochemically active sites (batteries, super capacitors) and energy conversion devices depending on catalytic sites or defect structures. NiO nanoparticles and their nanocomposites have been synthesized *via* a cost-effective and

highly convenient co-precipitation method [3]. Mn₂O₃ nanoparticles can be utilized for advanced materials in batteries, as well as other applications, such as water treatment and imaging contrast agents [4]. CdO has potential applications in flat panel displays, organic light emitting diodes, optoelectronic devices, gas sensors and electrodes [5]. CdO also possesses both antibacterial and anticancer activity. Previous studies reported the synthesis of nanocomposites containing CdO and other metal oxide combinations [6]. The Pb₂O₃ nanoparticles are used in magnetic resonance and as magnetic nanoparticles for magnetic data storage and magnetic resonance imaging (MRI). The most

common use of ZnO nanoparticles is in sunscreen, because they reflect ultraviolet light, but they are small enough to be transparent to visible light [7]. They are also being investigated to kill harmful microorganisms in packaging [8]. In this paper, nanocomposites of NiO were synthesized and their structural optical properties were analyzed.

2. Materials and Methods

In the present work, co-precipitation method is used to prepare NiO and their nanocomposites. All the precursors used for synthesis were of analytical grade (Merck). Pure nickel acetate, manganese acetate, cadmium acetate, lead acetate, zinc acetate, double distilled water, urea and ammonium hydroxide solution were used to synthesize NiO nanoparticles and their nanocomposites.

2.1 Synthesis of NiO Nanoparticles

Nickel acetate (0.25 M) is dissolved in double distilled water (100 ml) separately and stirred well for 30 minutes. Then, urea (0.75 M) is dissolved in double distilled water (100 ml) separately and stirred well. Then, both nickel acetate and urea solutions are mixed together. Ammonium hydroxide solution (32 M) is added drop by drop to maintain the pH of 10. The obtained green color precipitate is kept in the hot air oven at 100°C for drying. After grinding in agate mortar, the powder is kept in the muffle furnace at 400°C for 2 hours and the black color powder is obtained.

2.2 Synthesis of NiO Nanocomposites

Manganese acetate (0.25 M) is dissolved in double distilled water separately and stirred well for 30 minutes. Then, manganese acetate solution is added dropwise to the nickel acetate and urea solutions which are already mixed together. Ammonium hydroxide solution is added dropwise to maintain the pH of 10. The brown color precipitate is dried at 100°C in the hot air oven. After grinding the sample, it is kept in the muffle furnace at 400°C for two hours. Similar procedure is adopted for synthesizing other nanocomposites. In the place of manganese acetate, cadmium acetate is used for NiO-CdO nanocomposites, lead acetate is used for NiO-Pb₂O₃ nanocomposites and zinc acetate is used for NiO-ZnO nanocomposites.

3. Results and Discussion

3.1 PXRD Analysis

The powder X-Ray diffraction pattern of NiO nanoparticles and their nanocomposites were recorded using XPERT-PRO Diffraction system with CuK α radiation of wavelength 1.54056 Å. The PXRD patterns obtained for the NiO and their nanocomposites are shown in Fig.1 (a-e). The observed 2θ values were matched well with the cubic structure of NiO (JCPDS File No.89-5881) [9,10]. The relatively sharp and high intense diffraction peaks clearly indicate the crystalline nature of the synthesized pure NiO nanoparticles. The high intensity peaks are observed at (222), (400), (440) and (622) corresponding to $2\theta = 37.1979^\circ$, $2\theta = 43.1980^\circ$, $2\theta = 62.8085^\circ$ and $2\theta = 75.2708^\circ$, respectively. (Fig.1a) indicates the PXRD pattern of NiO nanoparticles. No peaks were observed from other impurities, such as Ni(OH)₂, indicating the high purity of the synthesized NiO nanoparticles.

Fig.1b portrays the XRD pattern of NiO-Mn₂O₃ nanocomposites. Diffraction peaks of both NiO and Mn₂O₃ were observed and matched with the standard JCPDS file (for Mn₂O₃ (JCPDS File No.71-0636) and NiO (JCPDS File No. 89-5881)). The material belongs to the cubic structure. The diffraction peaks are of low intensity when compared to the pure NiO nanoparticles (Fig.1b), which shows less crystallinity of NiO-Mn₂O₃ nanocomposites. The peaks of Mn₂O₃ are observed at (321), (440) corresponding to $2\theta = 35.7703^\circ$ and $2\theta = 63.4698^\circ$ respectively and the peaks of NiO are observed at (111), (222), (400), (511) and (622) corresponding to $2\theta = 18.4211^\circ$, $2\theta = 37.4112^\circ$, $2\theta = 43.5952^\circ$, $2\theta = 57.6035^\circ$ and $2\theta = 75.8341^\circ$, respectively.

In the NiO-CdO composites, both the diffraction peaks of the cubic phases were present for CdO (JCPDS File No. 05-0640) and NiO (JCPDS File No. 89-5881) [11]. The peaks of CdO are observed at (200), (220), (311) and (222) corresponding to $2\theta = 38.2483^\circ$, $2\theta = 55.2383^\circ$, $2\theta = 65.9156^\circ$ and $2\theta = 69.1591^\circ$, respectively and the peaks of NiO are observed at (111), (311), (400) and (440) corresponding to $2\theta = 32.9683^\circ$, $2\theta = 35.5949^\circ$, $2\theta = 43.1799^\circ$ and $2\theta = 63.0358^\circ$, respectively (Fig.1c). The NiO peak corresponding to (111) is of high relative intensity.

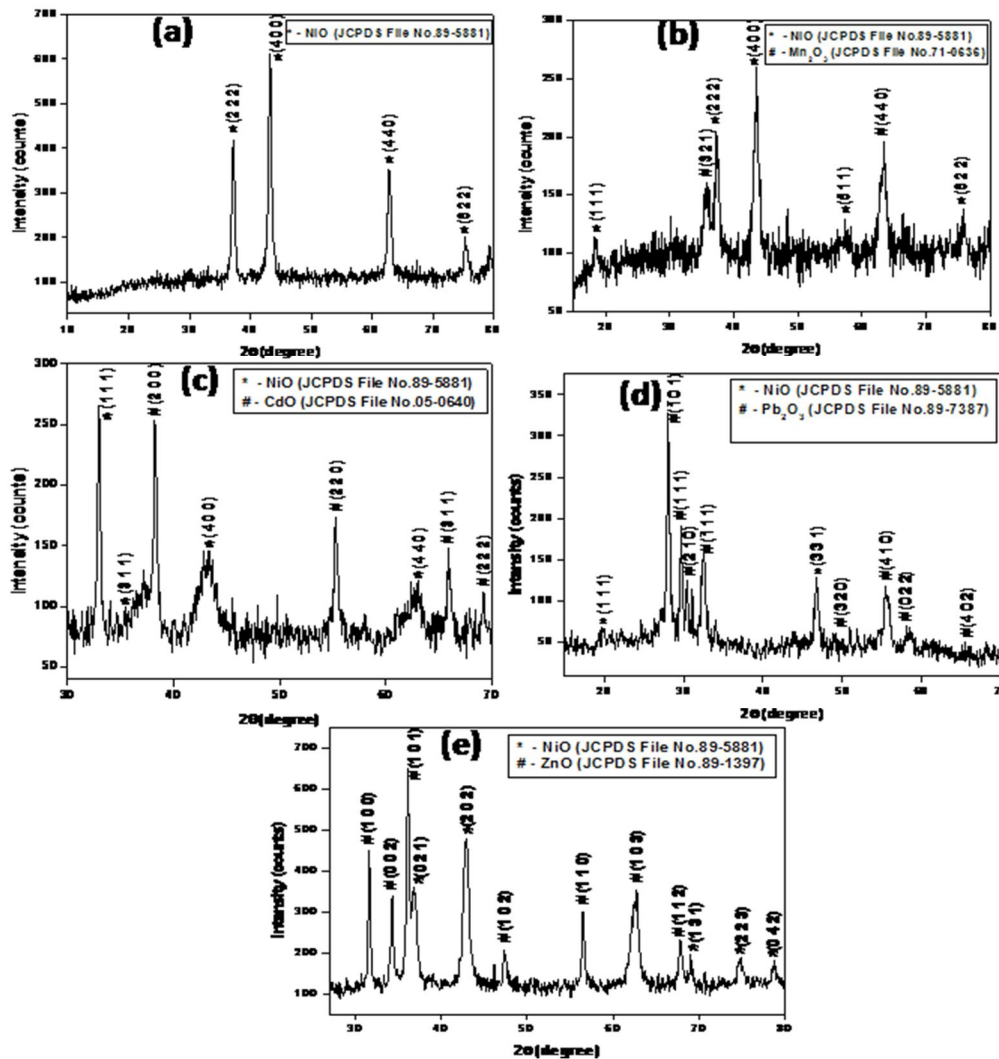


FIG. 1. PXRD pattern of a) NiO nanoparticles b) NiO-Mn₂O₃ nanocomposites c) NiO-CdO nanocomposites d) NiO-Pb₂O₃ nanocomposites e) NiO-ZnO nanocomposites.

The presence of monoclinic Pb₂O₃ (JCPDS File No.89-7387) and cubic NiO (JCPDS File No.89-5881) in the synthesized nanocomposites confirms the formation of NiO-Pb₂O₃ nanocomposites [12] (Fig.1d). The peaks of Pb₂O₃ are observed at (101), (111), (210), (020), (111), (320), (410), (022) and (402) corresponding to $2\theta = 28.0724^\circ$, $2\theta = 29.7112^\circ$, $2\theta = 30.4154^\circ$, $2\theta = 31.1061^\circ$, $2\theta = 32.5639^\circ$, $2\theta = 50.9270^\circ$, $2\theta = 55.2597^\circ$, $2\theta = 58.4788^\circ$ and $2\theta = 65.7442^\circ$, respectively and the peaks of NiO are observed at (111) and (331) corresponding to $2\theta = 19.9476^\circ$ and $2\theta = 46.7938^\circ$, respectively.

The presence of hexagonal ZnO (JCPDSFileNo.89-1397) and cubic NiO (JCPDSFile No.89-5881) in the synthesized nanocomposites confirms the formation of NiO-ZnO nanocomposites [13, 14]. The peaks of ZnO are observed at (100), (002), (101), (102), (110),

(103) and (112) corresponding to $2\theta = 31.6276^\circ$, $2\theta = 34.2888^\circ$, $2\theta = 36.1362^\circ$, $2\theta = 47.3647^\circ$, $2\theta = 56.4882^\circ$, $2\theta = 62.8006^\circ$ and $2\theta = 67.8877^\circ$, respectively and the peaks of NiO are observed at (021), (202), (131), (223) and (042) corresponding to $2\theta = 36.9005^\circ$, $2\theta = 42.7812^\circ$, $2\theta = 68.9920^\circ$, $2\theta = 74.6008^\circ$ and $2\theta = 78.6843^\circ$, respectively. More number of ZnO peaks are observed and the ZnO peak corresponding to (101) is of high relative intensity (Fig.1e).

The average grain size of synthesized Nickel Oxide nanoparticles is found out from the powder XRD pattern using Debye Scherrer's formula:

$$D = 0.9\lambda/\beta\cos\theta \text{ (nm)}$$

where λ is the wavelength of PXRD, β is the full width half maximum; θ is the Bragg's angle for the peak. The average size of NiO nanoparticles is found to be 30.1052 nm.

TABLE 1. Comparison of average grain size of nanopowder samples.

S.No.	Nanopowder samples	Angle 2θ (degree)	θ (degree)	FWHM β (degree)	Average grain size D (nm)
1	NiO	47.7348	23.8674	0.328	30.1052
2	NiO-Mn ₂ O ₃	48.1587	24.0793	0.5576	19.6660
3	NiO-CdO	48.0926	24.0463	0.2952	29.4914
4	NiO-Pb ₂ O ₃	34.2853	17.1426	0.2583	32.2104
5	NiO-ZnO	43.3364	21.6682	0.3075	27.8206

3.2 SEM and EDAX Analysis

In order to produce clearer, less electrostatically distorted images, Field Emission Scanning Electron Microscopy (FESEM) was used in the present work and the FESEM images of the NiO nanoparticles and their nanocomposites were obtained using a JEOL JSM – 6390 microscope operating at an accelerating voltage of 20 kV.

Particles of average size 250 nm were observed in the FESEM image of pure NiO nanoparticles at a magnification of 1 μm [15] (Fig.2a). The FESEM image of the NiO-CdO nanocomposites (Fig.2b) displays the particles

with an average size of 855 nm. Needle-shaped rod-like structure with an average size of 880 nm was observed for NiO-Pb₂O₃ nanocomposites at a magnification of 2 μm (Fig.2c). Fig.2d shows that the NiO-Mn₂O₃ nanocomposites contain spherical-shaped particles with an average size of 350 nm at a magnification of 1 μm . The spherical-shaped morphology is obtained for NiO-ZnO nanocomposites with an average size of 900 nm at a magnification of 30 μm (Fig.2e).

EDAX images (Fig. 3) show the formation of the respective elements present in the pure NiO nanoparticles and their nanocomposites.

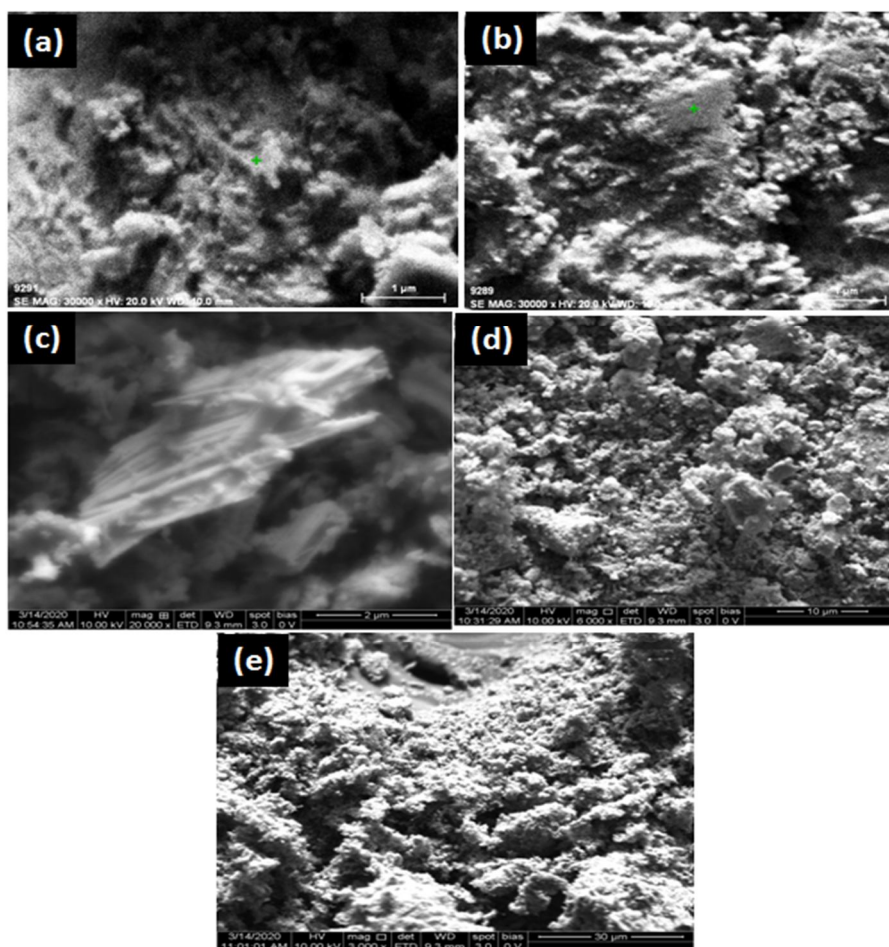


FIG. 2. FESEM image of a) NiO nanoparticles b) NiO-CdO nanocomposites c) NiO-Pb₂O₃ nanocomposites d) NiO-Mn₂O₃ nanocomposites e) NiO-ZnO nanocomposites.

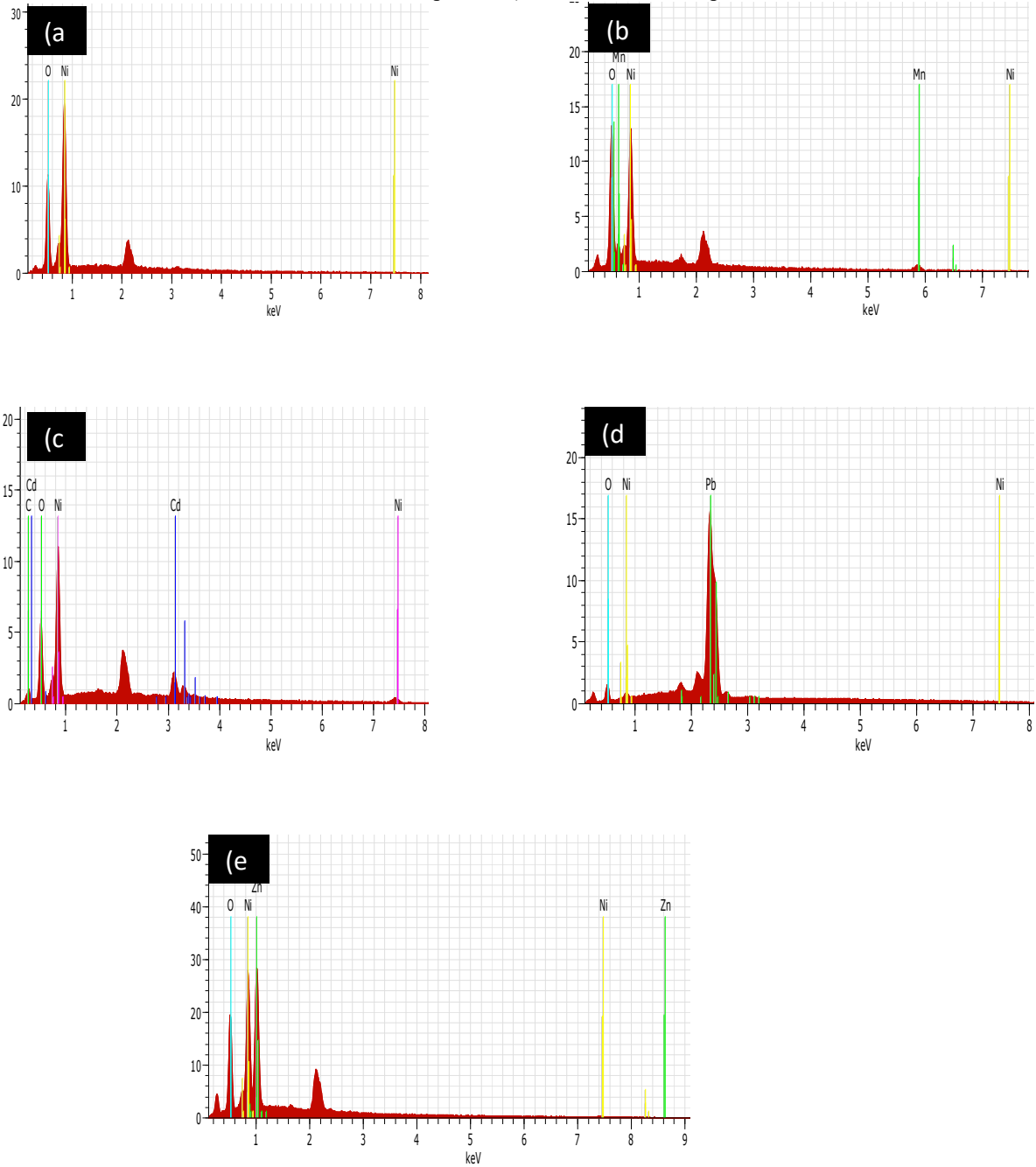


FIG. 3. EDAX image of a) NiO nanoparticles b) NiO-Mn₂O₃ nanocomposites c) NiO-CdO nanocomposites d) NiO- Pb₂O₃ nanocomposites e) NiO-ZnO nanocomposites.

3.2 Raman Analysis

Raman analysis is a spectroscopic technique used to observe vibrational, rotational and other low-frequency modes in a system. Raman spectroscopy is commonly used in chemistry to provide a structural fingerprint by which molecules can be identified.

Three Raman peaks of NiO located at 165, 510 and 1042 cm⁻¹ confirm the characteristic feature of NiO [16]. The band at 510 cm⁻¹ is attributed to one phonon (450 cm⁻¹) plus one magnon (60 cm⁻¹) excitation of NiO. The NiO-Mn₂O₃ nanocomposites show Raman peaks at 507cm⁻¹, 579 cm⁻¹ and 633 cm⁻¹. The intensity of the characteristic peak is found to be decreasing when compared to pure NiO nanoparticles. The

NiO-CdO nanocomposites show Raman peaks at 486 and 1012 cm^{-1} . The shift in band from 510 cm^{-1} to 486 cm^{-1} might be due to the decreased particle size compared to pure NiO nanoparticles [17]. The NiO-Pb₂O₃ nanocomposites show Raman peaks at 262 and 525 cm^{-1} . The peaks have different shift values and the intensity of the peak is found to be increasing when compared to the spectrum of pure NiO

nanoparticles. The NiO-ZnO nanocomposites show Raman peaks at 552 and 1058 cm^{-1} . This modification is probably due to the loss of lattice oxygen at high temperatures that leads to the surface reconstruction [18]. Generally, one phonon TO and LO modes of NiO would be observed at ~ 500 -570 cm^{-1} [19]. The band observed at 500-525 cm^{-1} symbolizes the presence of NiO.

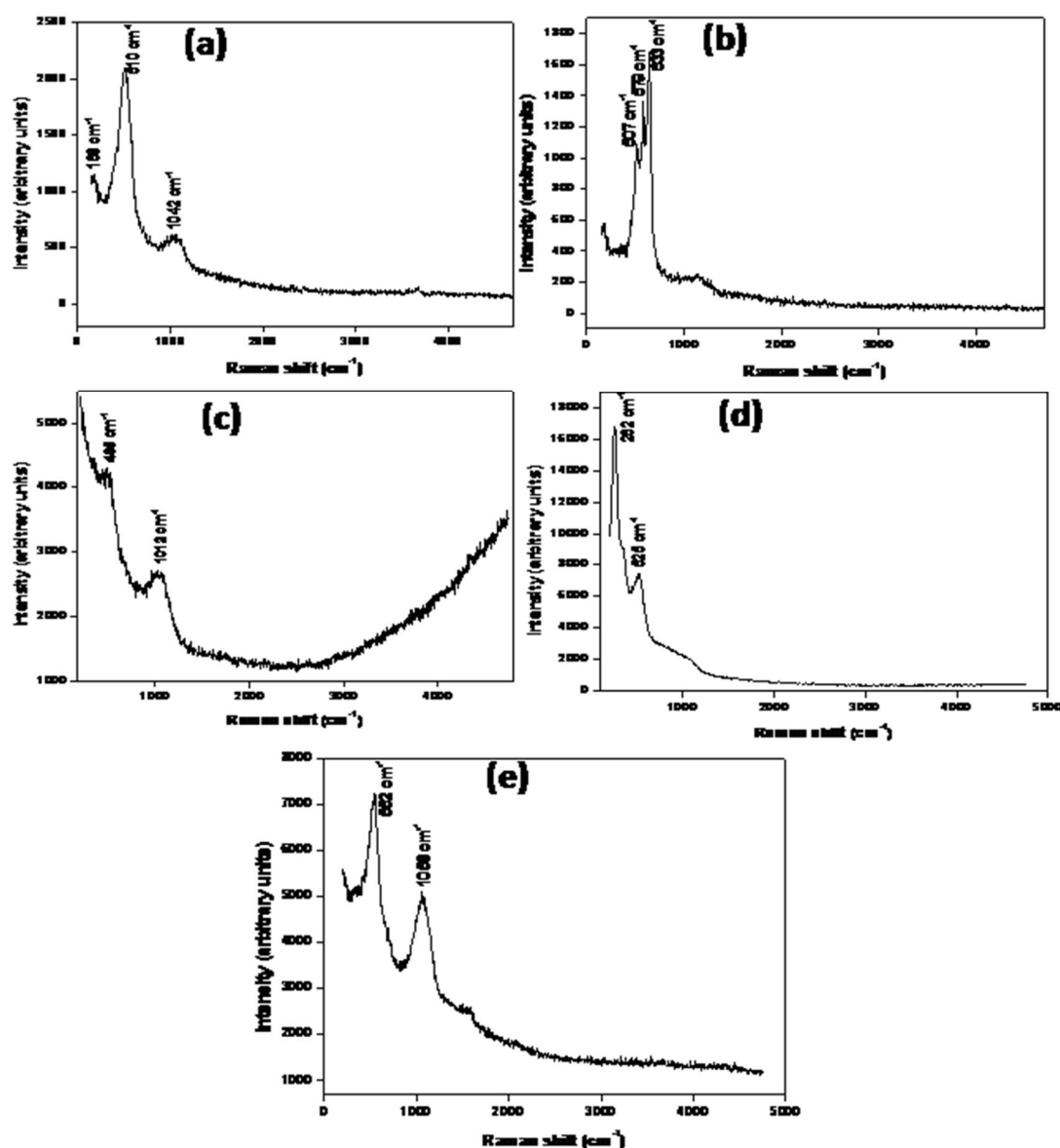


FIG. 4. Raman spectrum of a) NiO nanoparticles b) NiO-Mn₂O₃ nanocomposites c) NiO-CdO nanocomposites d) NiO- Pb₂O₃ nanocomposites e) NiO-ZnO nanocomposites.

3.3 Photoluminescent Analysis

Photoluminescence (PL) studies for the synthesized nanostructures were carried out using a photoluminescence spectrophotometer (Cary Eclipse) and the emission spectra were recorded at a scan rate of 600 nm/min using an excitation wavelength of 325nm.

Fig.5a depicts the photoluminescence (PL) emission spectrum and shows a maximum peak at 361 nm. High intense peaks centered at 361 nm are assigned to band edge emission of NiO nanocrystallites. The PL emission spectrum of NiO - Mn₂O₃ nanocomposites (Fig.5d) shows prominent peak at 360 nm. The PL emission

spectrum of NiO–CdO nanocomposites (Fig.5b) shows prominent peak at 491 nm. The intensity of the maximum peak is decreasing when compared to the pure NiO nanoparticles. The PL emission spectrum of NiO - Pb₂O₃ nanocomposites (Fig.5c) shows strong emission band at 491 nm close to the edge of the blue

region. The PL emission spectrum of NiO–ZnO nanocomposites (Fig.5e) which shows maximum peak at 491 nm is similar to Petronela et al.'s work on NiO-ZnO [20]. In the photoluminescent spectra, blue and green emission is observed in the NiO nanoparticle and their composites [21].

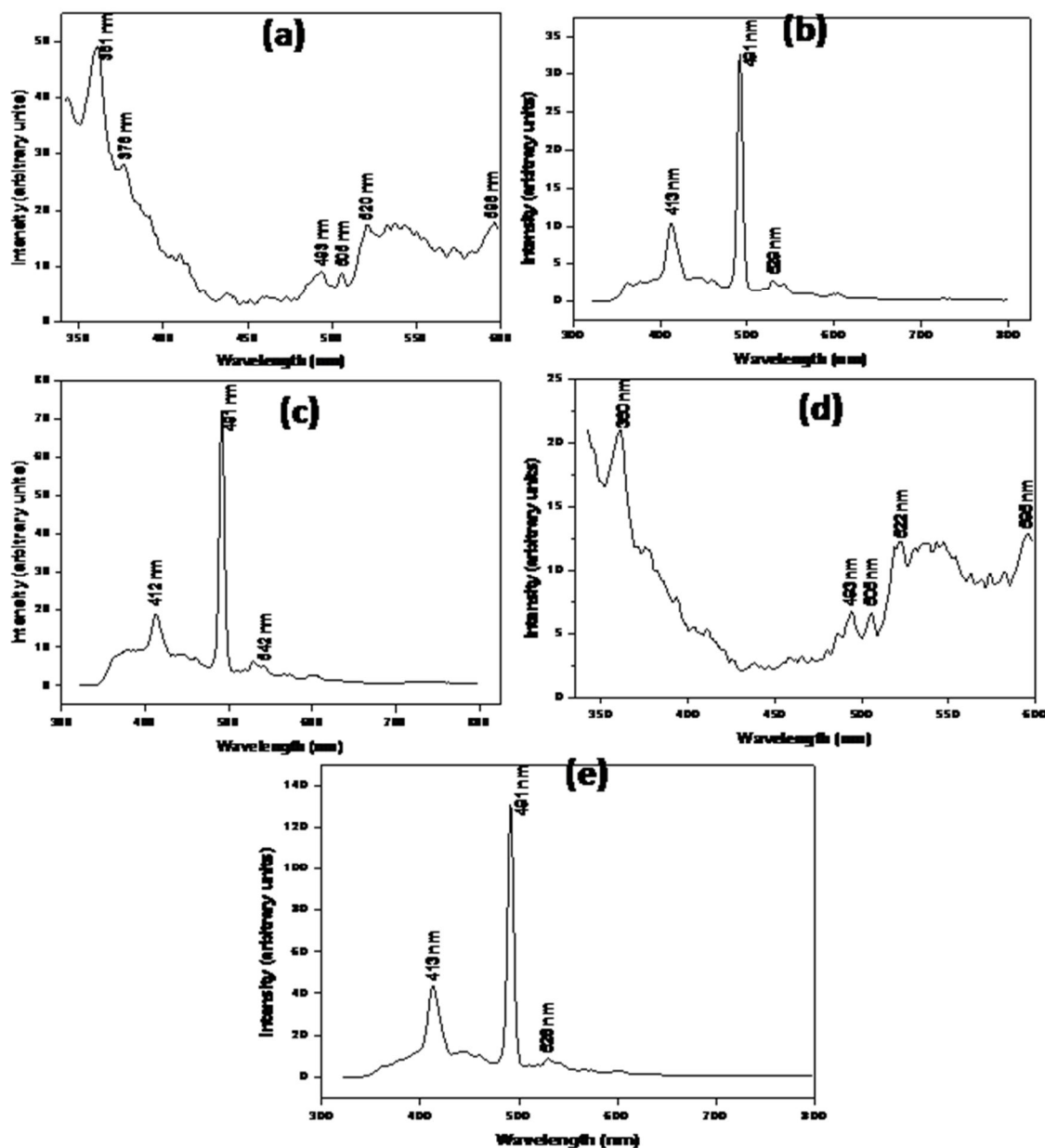


FIG. 5. PL spectrum of a) NiO nanoparticles b) NiO-CdO nanocomposites c) NiO-Pb₂O₃ nanocomposites d) NiO-Mn₂O₃ nanocomposites e) NiO-ZnO nanocomposites.

3.4 UV – Visible Analysis

To characterize the absorption properties of the synthesized samples, UV-Vis absorption spectrophotometer (Hitachi U-2900) was used at a scan speed of 400 nm/min in the range of 190 nm-800 nm.

It can be seen that the absorption edge corresponding to NiO appeared at 327 nm [22], the absorption edge corresponding to NiO-Mn₂O₃ appeared at 367 nm, the absorption edge corresponding to NiO-CdO appeared at 443 nm, the absorption edge corresponding to NiO-Pb₂O₃ appeared at 372 nm and the absorption edge

corresponding to NiO-ZnO appeared at 323 nm [23], respectively. There was blue shift absorbed in all the synthesized samples.

UV studies also support the blue emission of the synthesized NiO nanoparticles and nanocomposites.

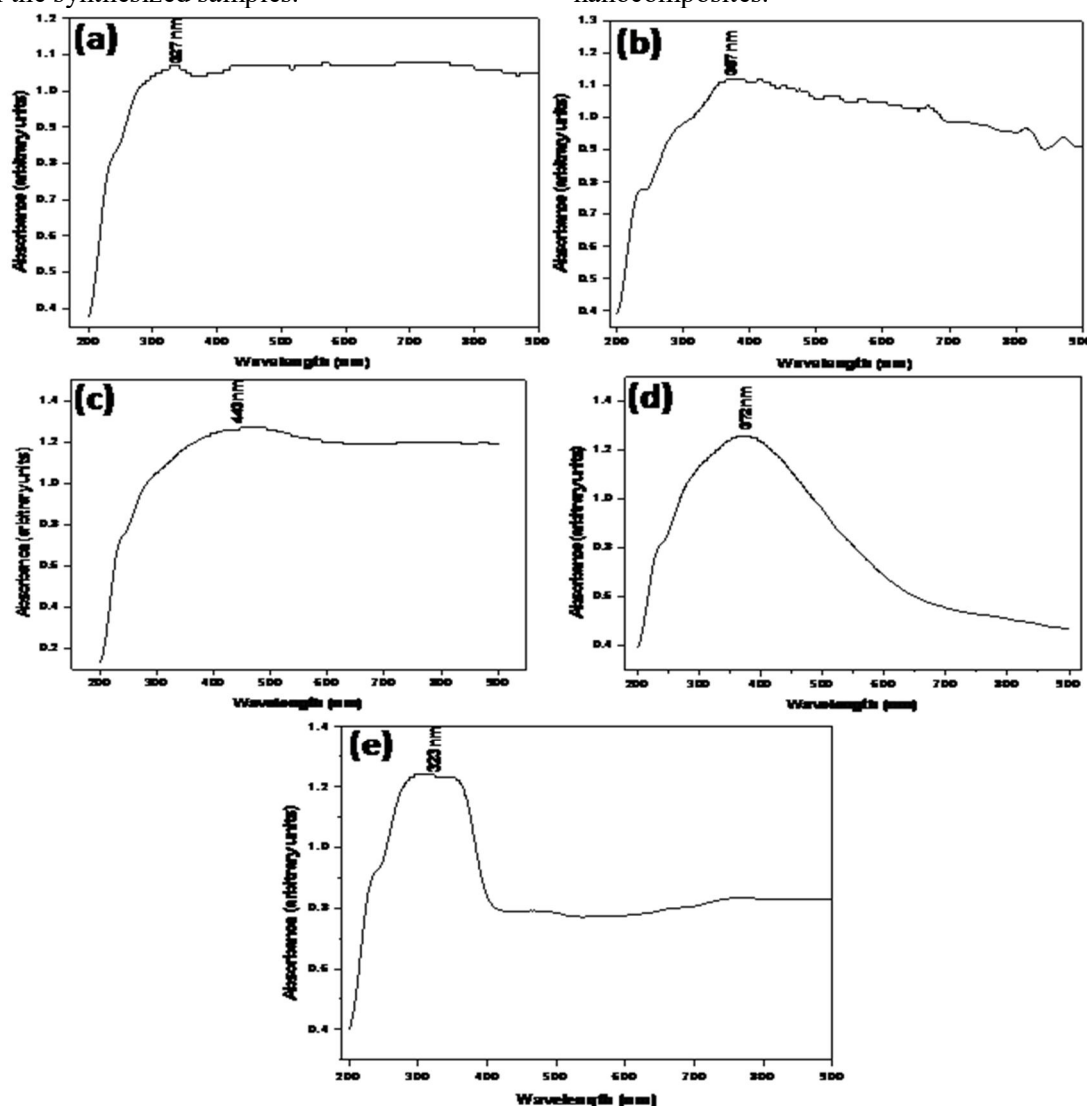


FIG. 6. UV-vis absorption spectrum of a) NiO nanoparticles b) NiO-Mn₂O₃ nanocomposites c) NiO-CdO nanocomposites d) NiO-Pb₂O₃ nanocomposites e) NiO-ZnO nanocomposites.

4. Conclusion

Co-precipitation method is used to synthesize pure NiO nanoparticles and their nanocomposites. PXRD and SEM studies confirmed the nanostructures for the prepared samples. The average size of NiO nanoparticles is found to be 30.1052 nm using Debye Scherer's formula. Spherical-shaped structure was obtained for NiO nanoparticles and their nanocomposites and needle-shaped rod-like structure was obtained for NiO-Pb₂O₃. The formation of NiO nanoparticles and their nanocomposites was confirmed by EDAX. Raman spectrum showed the characteristic peaks of pure NiO and their synthesized

nanocomposites. The PL study of NiO nanoparticles and their nanocomposites revealed the blue and green emissions. UV-vis spectra revealed the absorption edges corresponding to NiO at 327 nm, NiO- Mn₂O₃ at 367 nm, NiO-CdO at 443 nm, NiO-Pb₂O₃ at 372 nm and NiO-ZnO at 323 nm. Thus, the synthesized NiO nanocomposites are suitable for electrocatalysis application in future. Transition metal oxides have proved to be active in catalytic reactions and were used as good electrocatalysts as reported in literature. Since the nanocomposites of oxides Mn₂O₃, CdO, Pb₂O₃ and ZnO based on NiO are successfully synthesized; in future works, the synthesized samples can be further modified for electrocatalysis applications.

References

- [1] Xiaoming, F. and Zaizhi, Y., *Advanced Materials Research*, 228-229 (2011) 34.
- [2] Fu, S.-Y. and Liu, X.-M., *Progress in Solid State Chemistry Research*, 2007 (2007)165.
- [3] Kaur, N., Singh, J., Kaur, G., Kumar, S., Kukkar, D. and Rawat, M., *Micro and Macro Letters*, 14 (2019) 856.
- [4] Chen, H. and He, J., *J. Phys. Chem.*, 112 (2008) 17540.
- [5] Kumar, P.S., Selvakumar, M., Bhagabati, P., Bharathi, B., Karuthapandian, S. and Balakumar, S., *RSC Adv.*, 4 (2014) 32977.
- [6] Liu, B., Chew, C.H., Gan, L.M. and Xu, G.Q., *J. Mater. Res.*, 16 (2001) 1644.
- [7] Kessler, R., *Environmental Health Perspectives*, 119 (3) (2011) A120.
- [8] Iosub, C.S., Olareț, E., Grumezescu, A.M., Holban, A.M. and Andronescu, E., *Nanostructures for Novel Therapy*, Elsevier, 2017 (2017) 793.
- [9] Davar, F., Fereshteh, Z. and Salavati-Niasari, M., *J. Alloys Compd.*, 476 (2009) 797.
- [10] Zhu, J., Gui, Z., Ding, Y., Wang, Z., Hu, Y. and Zou, M., *J. Phys. Chem. C*, 111 (2007) 5622.
- [11] Karthik, K., Dhanuskodi, S., Gobinath, C., Prabukumar, S. and Sivaramkrishnan, S., *J. Phys. Chem. Solids*, 112 (2018) 106.
- [12] Aliakbari, A., Najafi, E., Amini, M.M. and Weng Ng, S., *Monatsh. Chem.*, 145 (2014) 1277.
- [13] Zhou, J., Zhao, F., Wang, Y., Zhang, Y. and Yang, L., *J. Lumin.*, 122-123 (1-2) (2007) 195.
- [14] Khoshhesab, Z.M., Sarfaraz, M. and Asadabad, M.A., *Synthesis and Reactivity in Inorganic, Metal-Organic and Nano-Metal Chemistry*, 41 (7) (2011) 814.
- [15] Khalaji, A.D. and Das, D., *International Nano Letters*, 4 (2014) 117.
- [16] Cordoba-Torresi, S.I., Hugot-Le Goff, A. and Joiret, S., *J. Electrochem. Soc.*, 138 (1991) 1554.
- [17] Mironova-Ulmane, N., *J. Phys.: Conf. Ser.*, 93 (2007) 012039.
- [18] Luo, Y., Deng, Y., Mao, W., Yang, X.-J., Zhu, K., Xu, J. and Han, Y.-F., *J. Phys. Chem. C*, 116 (39) (2012) 20975.
- [19] Sone, B.T., Fuku, X.G. and Maaza, M., *Int. J. Electrochem. Sci.*, 11 (2016) 8204.
- [20] Dorneanu, P.P., Airinei, A., Olaru, N., Homocianu, M., Nica, V. and Doroftei, F., *Mater. Chem. Phys.*, 148 (2014) 1029.
- [21] Riegel, G. and Bolton, J.R., *J. Phys. Chem.*, 99 (1995) 4215.
- [22] Dharmaraj, N., Prabu, P., Nagarajan, S., Kim, C.H., Park, J.H. and Kim, H.Y., *Mater. Sci. Eng. B*, 128 (2006) 111.
- [23] Mote, V.D., Purushotham, Y. and Dole, B.N., *Journal of Theoretical and Applied Physics*, 6 (6) (2012) 2251.